Optimal Transport Full Waveform Inversion - Applications

D. Carotti[1], O. Hermant[1], S. Masclet[1], M. Reinier[1], J. Messud[1], A. Sedova[1], G. Lambaré[1]

[1] CGG

Summary

While full waveform inversion (FWI) has imposed itself as a privileged velocity model building tool in areas investigated by diving waves, it is still penalized by its sensitivity to cycle skipping. Among the various strategies proposed to mitigate the problem, optimal transport (OT) FWI appears as one of the most successful industrial solutions. In order to illustrate this status, we review a set of marine and land applications of multi-dimensional (in data space, not to be confused with the velocity model dimensionality) OT-FWI. Compared to classical FWI, we confirm a relaxed sensitivity to cycle skipping with an additional update that goes deeper into the model (areas investigated by reflections) and provides improved structural consistency.

Introduction

Various solutions have been proposed to mitigate cycle skipping in Full Waveform Inversion (FWI) (Jiao et al., 2015; Warner and Guash, 2016; Wang et al., 2016; Poncet et al., 2018; Zhang et al., 2018). These solutions can lead to reliable industrial solutions and have already demonstrated their efficiency in various geological contexts. Among them, multi-dimensional (multiD) Optimal Transport (OT) FWI, (multiD in data space and not to be confused with the velocity model dimensionality) has been proposed by Métivier et al. (2016) and further studied by Poncet et al. (2018). This solution has proven to be particularly successful in an industrial context, especially for land FWI (Messud and Sedova, 2019; Sedova et al., 2019; Hermant et al., 2019). These successes can partly be explained by the use of wide azimuth (WAZ), large offset, broadband acquisitions and a dedicated processing workflow (Sedova et al., 2019). Comparison with conventional (least-squares, LS) FWI results clearly reveals that the use of multiD OT-FWI also contributes significantly to these successes (Messud and Sedova, 2019).

In this abstract, we present and analyze a set of land and marine applications. Firstly, a marine application on the Greater Castberg area, with a source over the streamer acquisition configuration. The comparison to the conventional LS-FWI results shows the mitigation of cycle skipping brought by multiD OT-FWI. Secondly, a land application on complex fault structures on-shore Oman, where we show that multiD OT-FWI can improve the delineation of complex velocity structures even below the maximum penetration depth of diving waves. The last example is a second land application from Oman, in an area proven to be particularly challenging for imaging, and even more for FWI (Perez-Solano and Plessix, 2019). It shows how multiD OT-FWI can be used jointly with a Multi-Wave Inversion (MWI), to better characterize the near surface.

MultiD OT FWI

Being more linear with respect to trace time shifts, OT distance offers an interesting opportunity for measuring the mismatch between observed and calculated traces in FWI. This has been highlighted by pioneers like Engquist et al. (2016) or Métivier et al. (2016). While OT distances were originally introduced to measure the cost of moving piles of sand, and more generally probability densities (with the associated positivity and mass conservation properties), they have been recast into more general formulations that can be applied to FWI, related to Wasserstein distances (Engquist et al., 2016). For example, while Wang and Wang (2019) use the 2-Wasserstein distance, Métivier et al. (2016) use a dual formulation of the 1-Wasserstein distance and include an additional constraint (this leads to the so-called Kantorovich-Rubinstein formulation). It is this second formulation, used here, that has been especially successful in industrial applications. Its main advantages are that:

- It can be used without a positive transformation of the traces (contrary to the classical OT formulation where a positivity constraint is requested).
- It exhibits a limited sensitivity to amplitude variations in the data.
- It can be efficiently implemented numerically, which allows for a tractable multiD (in data space) implementation.

We think that this last aspect is an important component especially in case of application to land data where the signal to noise ratio is often very low. Indeed, multi-dimensionality in the data space is an unusual property of OT-FWI misfits, which allows it to account for correlations between data samples in both the time and receiver directions. In contrast, LS-FWI is 0D in data space, meaning it considers each data sample independently and locally. In practice, the multi-dimensionality of OT-FWI results in an enhancement of the coherency of the events in the adjoint-source (or “residual”, that is back-propagated to obtain the velocity update), and thus to a more structurally consistent velocity update. More details are given in Messud and Sedova (2019).We now illustrate those advantages on various datasets.

A marine data example in Barents Sea

FWI in the Barents Sea is challenging because of gas accumulations of varying size and depth location. The example showed in Fig. 1 illustrates the stability of the multiD OT-FWI over the LS-FWI using the same input data (cleaned marine data, 8km offset maximum, same mute) and starting model. The automatic cycle skipping QC (normalised absolute value of the difference between observed and calculated data) allows for an analyzation of the model quality. Both LS-FWI and OT-FWI improve the

matching between observed and calculated data. However, OT-FWI shows far smaller "residual" time shifts compared to LS-FWI (see the red area on the left in Figure 1). Also, multiD OT-FWI converges to a more structurally consistent model, that is helped by the "multiD" property. Thus, even with a poor initial model, multiD OT-FWI delivers a robust velocity update and mitigates cycle skipping, whereas LS-FWI converge to a cycle-skipped model with poorer data matching and less structural consistency.

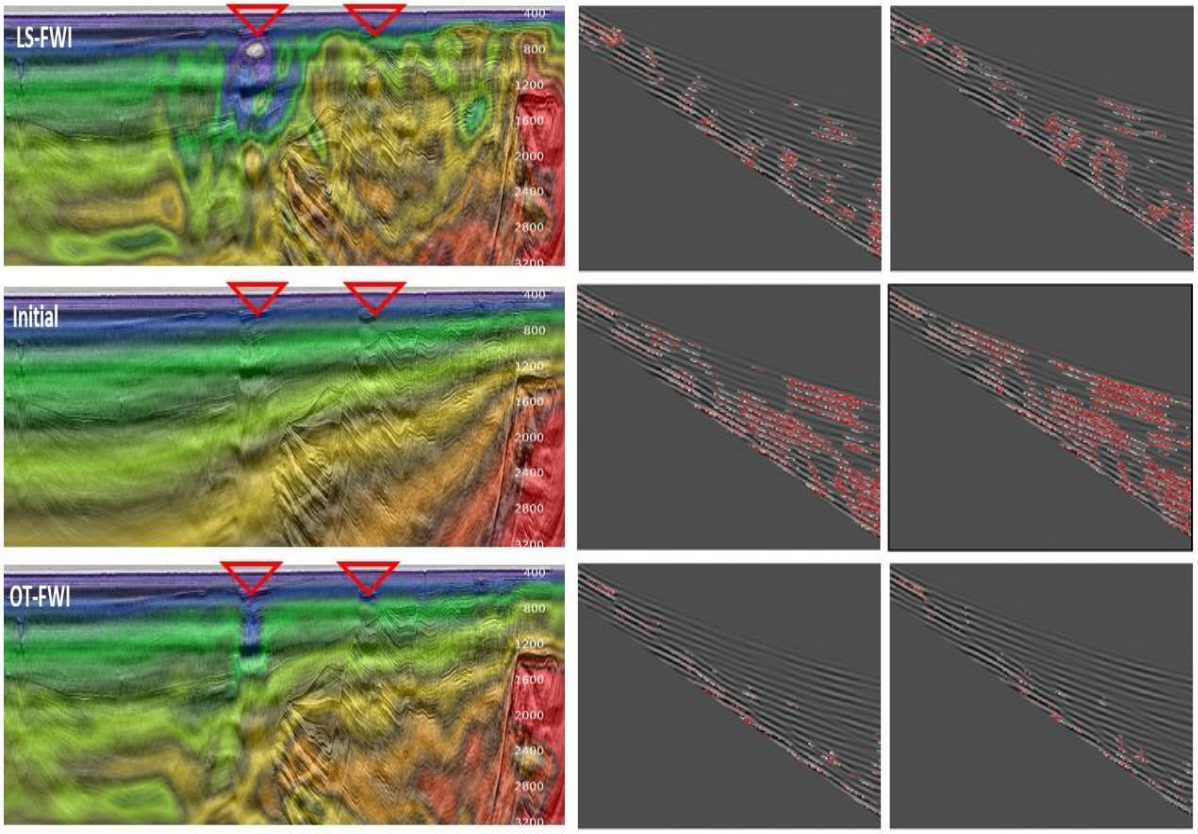

Figure 1: *Updated models at 7 Hz for LS-FWI (top left) and multiD OT-FWI (bottom left) starting from the same initial model (middle left). On the right we show the observed data (in black-grey-white) superimposed by red areas corresponding to locations where observed and modelled data have opposite sign and the misfit is bigger than a given threshold; dark red = high risk of cycle skipping.*

Land data with a complex faulted structure

The second application refers to a 3D land broadband dataset from the North of the Sultanate of Oman with full-azimuth and offsets of up to 13 km. This long-offset WAZ dataset was processed to enhance diving and post-critical waves. We ran FWI from a starting frequency of 2 Hz up to 16 Hz, following the workflow proposed by Sedova et al. (2019). Starting from a heavily smoothed VTI initial model obtained using a previous FWI result.

In Figure 2, we compare LS-FWI results to multiD OT-FWI results. The yellow oval in Figure 2c highlights the improved delineation of the velocity contrast at the top of the Gharif formation achieved by OT-FWI. The unexpected velocity increase obtained with LS-FWI at the base of the oval on Figure 2a is also corrected with OT-FWI, see Figure 2c. This improved velocity provides imaging uplifts of the deep reflectors observable in Figure 2d. Moreover, the focusing of the major fault, a difficult challenge for the area, is enhanced, as highlighted by the arrow in Figure 2d.

Land data with a shallow high velocity layer

The last application shown on Figure 3 is from the South of Oman. With the presence of the thin and shallow high velocity Rus layer, this area is a well-known challenge for land velocity model building and imaging. In particular, the use of acoustic FWI was challenged in this area (Perez Solano and Plessix, 2015, 2019). We show in this example that this difficulty can be overcome with a dedicated workflow, and an improved initial model for multiD OT-FWI update. A key to success is the

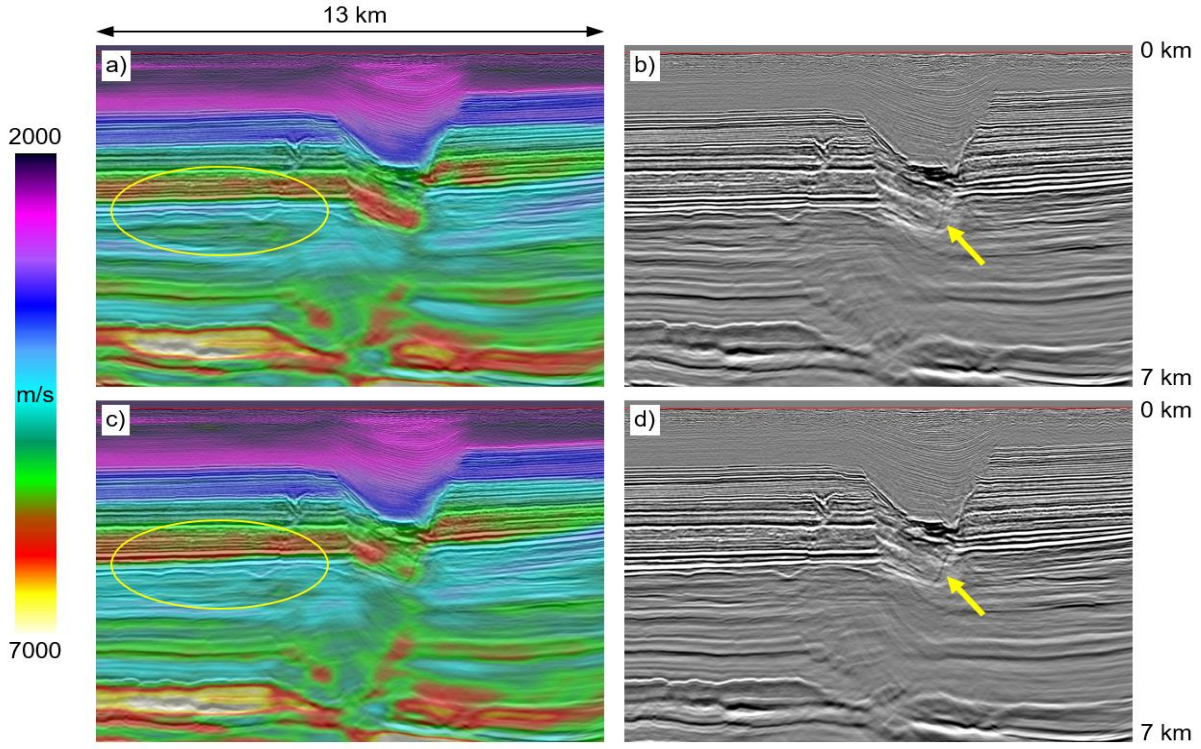

Figure 2: *FWI results on the North of Oman land data. a) LS-FWI velocity model superimposed on Kirchhoff depth migration (K-mig); b) K-mig image with LS-FWI model; c) MultiD OT-FWI velocity model superimposed on K-mig image; d) K-mig image with multiD OT-FWI.*

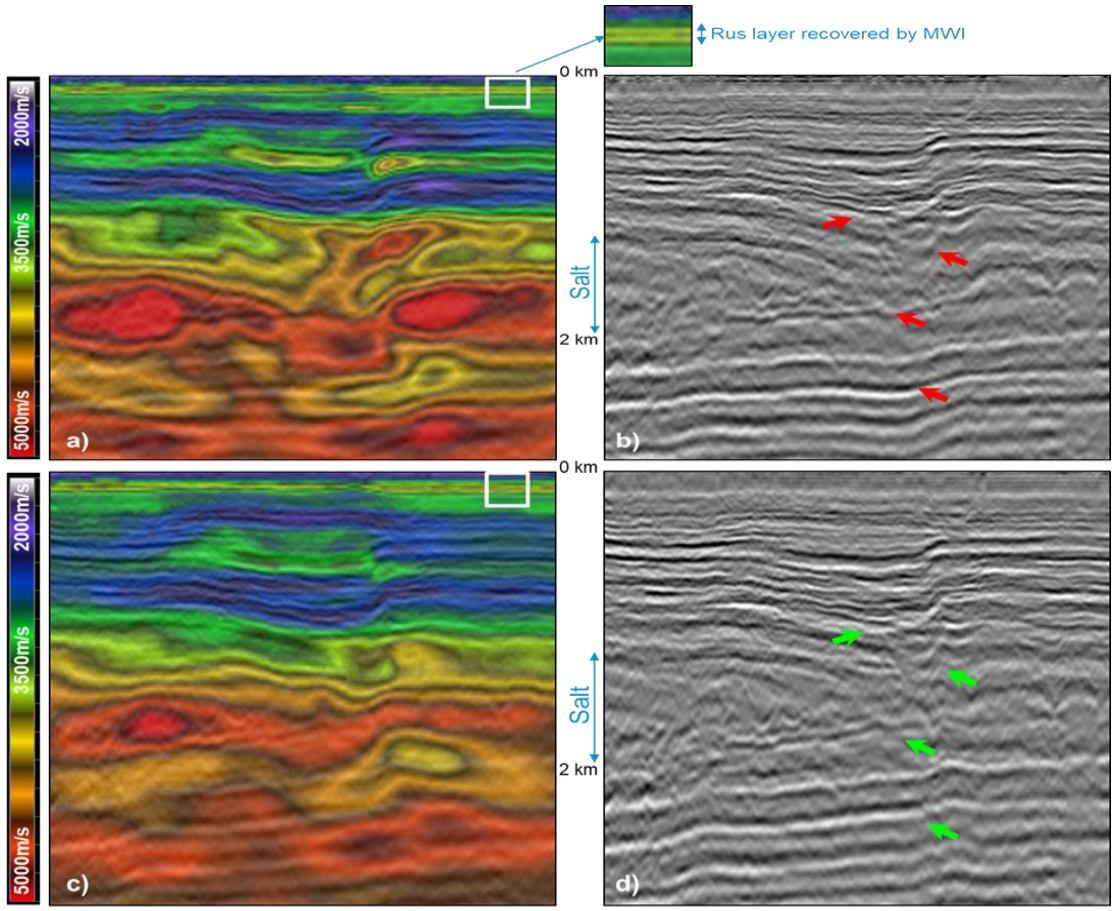

Figure 3: *7 Hz FWI results on the South of Oman land data. a) LS-FWI velocity model superimposed on RTM stack; b) RTM image with LS-FWI model; c) MultiD OT-FWI velocity model superimposed on RTM image; d) RTM image with multiD OT-FWI.*

inclusion of a near-surface model which was derived using multi-wave inversion (MWI) (Masclet et al., 2019), which allows inserting some key multiple generators at top and base of the anhydrite Rus layer. Figures 3c and 3d show that the combination of the MWI model and multiD OT-FWI (with reduced sensitivity to cycle-skipping) produces a geologically conformable velocity model and an improved migrated image in an area which would suffer from cycle-skipping issues if using LS-FWI (Figures 3a and 3b).

Conclusions

Among all of the FWI extensions proposed to mitigate cycle-skipping, multiD OT-FWI has proved quite promising with regards to successful applications in the context of wide azimuth broadband land datasets. We have presented here a set of new applications where it solves the challenges of acoustic FWI in the South of Oman notoriously challenging for acoustic FWI (Perez-Solano and Plessix, 2019) and also reveals its potential on marine data.

Acknowledgements

We are grateful to CGG Multi Client and New Ventures and PGS (example 1), PDO (example 2), OXY (example 3) and the Ministry of Oil and Gas of the Sultanate of Oman (examples 2 and 3) for providing data and permission to present these results.

References

Engquist, B., Froese, B. D. and Yang, Y. [2016] Optimal transport for seismic full waveform inversion. *Communications in Mathematical Sciences*, 14, 2309–2330.

Hermant, O., Sedova, A., Royle, G., Retailleau, M., Messud, J., Lambaré, G., Al Abri, S. and Al Jahdhami, M. [2019] Broadband FAZ land data: an opportunity for FWI. *81st EAGE Conference and Exhibition*, Extended abstract, WS08.

Jiao, K., Sun, D., Cheng, X. and Vigh, D. [2015] Adjustive full waveform inversion. *SEG Technical Program Expanded Abstracts*, 1091–1095.

Masclet, S., T. Bardainne, V. Massart and Prigent, H. [2019] Near Surface Characterization in Southern Oman: Multi-Wave Inversion Guided by Machine Learning, *81st EAGE Conference and Exhibition*, Extended abstract, Tu R16 05

Messud, J. and Sedova, A. [2019] Multidimensional Optimal Transport for 3D FWI: Demonstration on Field Data. *81st EAGE Conference and Exhibition*, Extended abstract, Tu R08 02.

Métivier, L., Brossier, R., Mérigot, Q., Oudet, E. and Virieux, J. [2016] Measuring the misfit between seimograms using an optimal transport distance: Application to full waveform inversion. *Geophysical Journal International* 205, 345-377.

Pérez Solano, C. A. and Plessix, R.-E. [2015], Elastic waveform inversion with modified surface boundary conditions for land seismic data: 77th *EAGE Conference and Exhibition*, Extended Abstracts, We N104 06.

Pérez Solano, C. and Plessix, R.-E. [2019] Velocity-model building with enhanced shallow resolution using elastic waveform inversion - An example from onshore Oman. *Geophysics*, 84, 6.

Poncet, R., Messud, J., Bader, M., Lambaré, G., Viguier, G. and Hidalgo, C. [2018] FWI with optimal transport: a 3D implementation and an application on a field dataset. *80th EAGE Conference and Exhibition*, Extended abstract, We A12 02.

Sedova, A., Messud, J., Prigent, H., Masclet, S., Royle, G. and Lambaré, G. [2019] Acoustic Land Full Waveform Inversion on a Broadband Land Dataset: the Impact of Optimal Transport. *81st EAGE Conference and Exhibition* Extended abstract, Th R08 07.

Wang, M., Xie, Y., Xu, W. Q., Xin, K. F., Chuah, B. L., Loh, F. C., Manning, T. and Wolfarth, S. [2016] Dynamic-warping full-waveform inversion to overcome cycle skipping. *86th SEG Annual International Meeting*, Expanded abstract, 1273-1277.

Wang, D. and Wang, P. [2019] Adaptive quadratic Wasserstein full-waveform inversion. *89th SEG Annual International Meeting*, Expanded abstract, 1300-1304.

Warner, M. and Guash, L. [2016] Adaptive waveform inversion: Theory. *Geophysics*, 81, R429–R445.

Zhang, Z., Mei, J., Lin, F., Huang, R. and Wang, P. [2018] Correcting for salt misinterpretation with full-waveform inversion. *88th SEG Annual International Meeting*, Expanded abstract, 1143-1147.